Medullary Breast Carcinoma, a Triple-Negative Breast Cancer Associated with BCLG Overexpression

Romero P, Benhamo V, Deniziaut G, Fuhrmann L, Berger F, Manié E, Bhalshankar J, Vacher S, Laurent C, Marangoni E, Gruel N, MacGrogan G, Rouzier R, Delattre O, Popova T, Reyal F, Stern MH, Stoppa-Lyonnet D, Marchiò C, Bièche I, Vincent-Salomon A.

Medullary Breast Carcinoma, a Triple-Negative Breast Cancer Associated with BCLG Overexpression.

Am J Pathol. 2018 Oct;188(10):2378-2391. doi: 10.1016/j.ajpath.2018.06.021.

MEDULLARY BREAST CARCINOMA, A TRIPLE-NEGATIVE BREAST CANCER ASSOCIATED WITH BCLG OVEREXPRESSION

Romero P[1], Benhamo V[2], Deniziaut G[3], Fuhrmann L[4], Berger F[5], Manié E[6], Bhalshankar J[6], Vacher S[7], Laurent C[8], Marangoni E[8], Gruel N[2], MacGrogan G[9], Rouzier R[10], Delattre O[6], Popova T[6], Reyal F[11], Stern MH[4], Stoppa-Lyonnet D[12], Marchiò C[13], Bièche I[14], Vincent-Salomon A[4].

1 Department of Pathology, Institut Curie, PSL Research University, Paris, France. Electronic address: pierre.romero@curie.fr. 2 INSERM U934, Institut Curie, PSL Research University, Paris, France; Department of Translational Research, Institut Curie, PSL Research University, Paris, France. 3 Department of Pathology, Institut Curie, PSL Research University, Paris, France. 4 Department of Pathology, Institut Curie, PSL Research University, Paris, France; INSERM U934, Institut Curie, PSL Research University, Paris, France. 5 Unit of Biometry, INSERM U900, Institut Curie, PSL Research University, Paris, France. 6 INSERM U934, Institut Curie, PSL Research University, Paris, France. 7 Pharmacogenomics Unit, Department of Genetics, Institut Curie, PSL Research University, Paris, France. 8 Department of Translational Research, Institut Curie, PSL Research University, Paris, France. 9 Department of Biopathology, Institut Bergonié, Bordeaux, France. 10 Department of Surgery, Institut Curie, PSL Research University, Paris, France. 11 Department of Translational Research, Institut Curie, PSL Research University, Paris, France; Department of Surgery, Institut Curie, PSL Research University, Paris, France. 12 Department of Pathology, Institut Curie, PSL Research University, Paris, France; INSERM U934, Institut Curie, PSL Research University, Paris, France; Sorbonne Paris Cité, University Paris Descartes, Paris, France. 13 Department of Pathology, Institut Curie, PSL Research University, Paris, France; Institute of Pathology at the Department of Medical Sciences, University of Turin, Turin, Italy. 14 Pharmacogenomics Unit, Department of Genetics, Institut Curie, PSL Research University, Paris, France; EA 7331, University Paris Descartes, Paris, France.

Abstract

Medullary breast carcinoma (MBC) is a rare subtype of triple-negative breast cancer with specific genomic features within the spectrum of basal-like carcinoma (BLC). In this study of 19 MBCs and 36 non-MBC BLCs, we refined the transcriptomic and genomic knowledge about this entity. Unsupervised and supervised analysis of transcriptomic profiles confirmed that MBC clearly differs from non-MBC BLC, with 92 genes overexpressed and 154 genes underexpressed in MBC compared with non-MBC BLC. Immunity-related pathways are the most differentially represented pathways in MBC compared with non-MBC BLC. The proapoptotic gene BCLG (official name BCL2L14) is by far the most intensely overexpressed gene in MBC. A quantitative RT-PCR validation study conducted in 526 breast tumors corresponding to all molecular subtypes documented the specificity of BCLG overexpression in MBC, which was confirmed at the protein level by immunohistochemistry. We also found that most MBCs belong to the immunomodulatory triple-negative breast cancer subtype. Using pan-genomic analysis, it was found that MBC harbors more losses of heterozygosity than non-MBC BLC. These observations corroborate the notion that MBC remains a distinct entity that could benefit from specific treatment strategies (such as deescalation or targeted therapy) adapted to this rare tumor type.

Introduction

Previous article in issueNext article in issue

Medullary breast carcinoma (MBC) is a rare morphologic subtype of invasive breast cancer, accounting for approximately 2% of invasive breast cancer.1 Most MBC belongs to the immunohistochemical (IHC) subgroup of triple-negative breast cancer (TNBC), and at the transcriptomic level, MBC usually displays basal-like genetic features.2 In previous studies, we found that, although it shares common genomic alterations with non-MBC basal-like carcinoma (BLC), MBC is a distinct genomic entity within the BLC spectrum, harboring a higher rate of TP53 mutations.3, 4 Moreover, the prognosis of MBC appears to be slightly better than that of grade-matched invasive carcinoma of no special type, despite its aggressive histopathologic features.5 To define more clearly the molecular events that characterize MBC as a morphologic and genomic subgroup of BLC, we performed a comprehensive retrospective study comparing MBC with non-MBC BLC through a transcriptomic analysis and a more detailed genomic analysis than in our previous work.3

Materials and Methods

Patients, Tumors, Cell Lines, and Xenografts

Tumors were retrospectively selected from two groups of patients on the basis of the availability of frozen samples and formalin-fixed, paraffin-embedded samples for determination of transcriptomic and genomic profiles and IHC, respectively. Samples with <50% of tumor cells were excluded from the study. The first group consisted of 19 MBCs, and the second group consisted of 36 grade III non-MBC BLCs (retrieved from Institut Curie Paris and Institut Bergonié in France). Experiments were performed in accordance with the French Bioethics Law 2004-800 and the National Institute of Cancer Ethics Charter. Morphologic and IHC assessments of diagnostic criteria in MBC were performed as previously described, in accordance with the criteria defined by Ridolfi et al.3, 6 Non-MBC BLC was defined using morphology and IHC as follows: absence of MBC morphologic criteria and lack of expression of estrogen receptor (ER), progesterone receptor (PR), and HER2 (ie, triple-negative phenotype), with the expression of at least one of the following markers: keratin 5/6, keratin 14, epidermal growth factor receptor, and KIT. Tumor-infiltrating lymphocytes (TILs) assessment in non-MBC BLC was performed by two independent readers (P.R., C.M.) as recommended by Salgado et al.7 Clinicopathological data are detailed in Supplemental Table S1.

Transcriptomic data validation analysis was performed with RNA tumor samples extracted from a series of 526 primary unilateral invasive breast tumors (retrieved from Institut Curie, Paris, France) between 1978 and 2008. Complete clinical, histologic, and laboratory data were available. Patients were managed by primary tumor excision without neoadjuvant chemotherapy or radiotherapy. ER, PR, and HER2 protein status was determined by biochemical methods (dextran-coated charcoal method, enzyme immunoassay, or IHC) and was confirmed by real-time quantitative RT-PCR (RT-qPCR) assays. The population was divided into four groups that reflected the intrinsic molecular classification: two luminal subtypes, luminal A [HR+ (ER+ or PR+)/HER2− (n = 295)] and luminal B [HR+ (ER+ or PR+)/HER2+ (n = 58)]; HER2+ subtype [HR− (ER− and PR−)/HER2+ (n = 72)]; and triple-negative (TN) subtype [HR− (ER− and PR−)/HER2− (n = 101)]. Sixteen normal breast tissue specimens from women undergoing cosmetic breast surgery were used as sources of normal RNA.

For validation of the gene of interest, 38 RNA samples extracted from cell lines obtained from the ATCC (Manassas, VA) were tested: seven nontumor cell lines, 17 TN tumor cell lines, 10 ER+ tumor cell lines, and 4 HER2+ cell lines (Supplemental Table S2). Transcriptomic findings were also validated on 61 RNA tumor samples extracted from patient-derived xenografts (PDXs) derived from 41 TNBCs, 15 ER+ carcinomas, and 5 HER2+ carcinomas. No PDXs were derived from MBC.

RNA and DNA Extractions

RNA was extracted using the RNeasy kit (Qiagen, Courtaboeuf, France), followed by the RNA cleanup kit (Macherey-Nagel, Hoerdt, France). The quality of each RNA sample was measured with an Agilent 2100 bioanalyzer (RNA integrity number >7), and the quantity of RNA was measured by spectrophotometry at 260 nm. For the transcriptomic analysis validation set, comprising 526 breast tumors, cell lines, and PDXs, total RNA was extracted from samples using acid-phenol guanidium as previously described.8 RNA quality was determined by electrophoresis on agarose gels, ethidium bromide staining, and visualization of the 18S and 28S RNA bands in UV light. DNA extraction and preparation for microarray experiments were performed by the Institut Curie Biological Resource Center. Before DNA isolation, a tissue section of tumor fragments was sampled and stained with hematoxylin and eosin to evaluate tumor cellularity. DNA was extracted from frozen tumor samples using a standard phenol/chloroform procedure. The quality of DNA was assessed on agarose gel. When a smear was observed instead of a band, the sample was discarded.

Gene Expression Analysis

Gene expression analysis was performed on 19 MBCs and 35 of 36 non-MBC BLCs. The RNA microarray used in this study was the GeneChip Human Genome U133 Plus 2.0 Array (Affymetrix, Santa Clara, CA), containing 54,613 probe sets. The transcriptomic data discussed in the present article, in addition to the genomic data from Affymetrix Genome Wide Human SNP Array 6.0 , have been deposited in the National Center for Biotechnology Information Gene Expression Omnibus (https://www.ncbi.nlm.nih.gov/geo; accession number GSE114269). Microarray data were simultaneously normalized using the GC robust multiarray average package 1.2 in the R environment (R Development Core Team). In this study, expression data were used to determine correlations between the genomic status of genes and their level of expression by comparing the log2 expression signal and the DNA copy number signal using Pearson's correlation test. A correlation between expression levels with respect to DNA copy number was considered significant when $R > 0.4$ and $P < 0.05$. Supervised analysis was performed to measure differential gene expression between MBC and non-MBC BLCs using a two-sided Welch t-test with $P < 0.05$ fold change >3. Partek GS software version 6.5 build 6.10.1020 (Partek Inc., St. Louis, MO) was used to generate unsupervised hierarchical clustering of expression data (Ward's method with Euclidean distance). Mean linkage was based on Pearson's dissimilarity of the 679 microarray probe sets with an interquartile range >3. A gene ontology–based determination of the biological pathways implicating differentially expressed genes in MBC and non-MBC BLC was performed using PANTHER pathway classification system version 13.0 (GENEONTOLOGY Unifying Biology, http://www.pantherdb.org, last accessed April 30, 2018), with the use of the Bonferroni correction for multiple testing.9

RT-qPCR for BCLG Expression

BCLG expression level was assessed in 19 MBCs, 41 non-MBC BLCs (34 from the initial cohort of 36 cases and seven additional samples collected previously with RNA available), 526 breast cancers corresponding to all molecular subtypes, 38 cell lines, and 61 PDXs. Quantitative values were obtained from the cycle number (CT value) at which the increase in the fluorescence signal associated with exponential growth of PCR products started to be detected by the laser detector of the ABI Prism 7900 sequence detection system (Perkin-Elmer Applied Biosystems, Foster City, CA), using Perkin-Elmer Applied Biosystems analysis according to the manufacturer's manuals. Because the precise amount of total RNA added to each reaction mix (based on optical density) and its quality (ie, lack of extensive degradation) are difficult to assess, we also quantified transcripts of the TBP gene (GenBank accession number NM_003194) encoding the TATA box-binding protein (a component of the DNA-binding protein complex TFIID) as an endogenous RNA control and normalized each sample on the basis of its TBP content.10 Results, presented as N-fold differences in BCLG gene expression relative to the TBP gene and termed NBCLG, were determined as NBCLG = $2\Delta CT$ sample, where the ΔCT value of the sample was determined by subtracting the CT value of the BCLG gene from the CT value of the TBP gene. The NBCLG values of the human tumor samples were subsequently normalized so that the median of the NBCLG values for the 16 normal breast tissues was equal to 1. The results were represented as follows: transcript level ≥ 3 was considered to indicate overexpression, and transcript level ≤ 0.33 was considered to indicate underexpression. Because no normal equivalent counterpart was available, the NBCLG values of the cell lines and PDX samples were subsequently normalized considering 1 to be the lowest quantifiable transcript level (CT = 35). The primers for TBP and BCLG (human and/or murine, long and short isoforms for BCLG) were chosen with the assistance of the Oligo 6.0 program (National Biosciences, Plymouth, MN). Overexpression of BCLG was defined as a BCLG expression level (NBCLG) >4. The dbEST and nr databases were scanned to confirm the total gene specificity of the nucleotide sequence chosen for the primers and the absence of single-nucleotide polymorphisms (SNPs). The nucleotide sequences of the oligonucleotide hybridization primers are given in Table 1. To avoid amplification of contaminating genomic DNA, one of the two primers was placed at the junction between two exons or on two different exons. Agarose gel electrophoresis was used to verify the specificity of PCR amplicons. The conditions of cDNA synthesis and PCR were as previously described.11BCLG gene transcription leads to three different transcripts. Two of them, differing from each other in terms of 5′-UTR configuration, led to the same protein after translation, the long variant of BCLG (BCLG-L). The third transcript encodes for the short variant of BCLG (BCLG-S). To document which of the variants is expressed in breast cancer, the BCLG gene expression level was compared in 19 MBCs and 21 breast tumors from the cohort of 526 samples considered to be high expressers, using primer pairs specific to long and short variants of BCLG in a RT-qPCR assay.

Genomic Alteration Analysis

SNP mapping assays were performed according to the manufacturer's protocol (Affymetrix, Santa Clara, CA). Briefly, 250 ng of genomic DNA from 19 MBCs and 36 non-MBC BLCs were digested with both Nsp and Sty restriction enzymes in independent parallel reactions, ligated to the adaptors, and amplified by PCR using a universal primer. After purification of PCR products with SNP clean magnetic beads (Agencourt Bioscience, Beverly, MA), amplicons were quantified, fragmented, labeled, and hybridized to Affymetrix Genome-Wide Human SNP 6.0 array. Targets were prepared when 45 μg of amplified DNA was available and when the target size was situated between 250 and 2000 bp and were then hybridized according to the manufacturer's recommendations. After washing and staining, the arrays were scanned to generate .cel files for downstream analysis. Normalization was performed using a Genotyping console (GenomeWideSNP_6.hapmap270.na31.r1.a5.ref)

provided by Affymetrix (GTC3.0.1). Genomic alterations were evaluated according to the Genome Alteration Print (GAP) method.12 Copy number and allelic content profiles were detected for each tumor based on the overall pattern of alterations, as previously described and validated.12 The cutoffs for alteration events (gains, losses, focal amplifications) were adapted according to the inferred ploidy. For near-diploid tumors, the genomic region with inferred copy number ≤ 1 or ≥ 3 and ≥ 6 were considered to be regions of loss, gain, and focal amplification, respectively. For near-tetraploid tumors, the copy number cutoffs used to define regions of loss, gain, and focal amplification were 2, 6, and 8, respectively. The minimum regions of amplification covering at least 25 consecutive SNPs with the same copy number status were considered to be recurrent regions when the frequency of alterations was >15% in the tumor samples tested, after exclusion of genomic variants according to the genomic variants database. Tumor profiles were visualized with GAP software (Institut Curie).12

Affymetrix Genome-Wide Human SNP Array 6.0 genomic data allowed the assessment of large-scale state transition (LST) status as described previously.13 Briefly, the LST score is the number of breakpoints between regions longer than 10 Mb after filtering out regions shorter than 3 Mb. Different cutoffs for the LST score were introduced for near-diploid and near-tetraploid tumors to separate BRCA1/2 intact and deficient samples, regardless of the inactivation process. This process resulted in segregation of samples into high LST and low LST samples according to the LST score. The LST status was able to be assessed in 16 of 19 MBCs and 34 of 36 non-MBC BLCs.

Methylation of the BRCA1 promoter was assessed by methyl-specific PCR after bisulfite conversion using the MethylDetector Kit (Active Motif, Carlsbad, CA), as previously described.14 Somatic and germline BRCA1/2 mutational status was determined as previously described.13 Primer sequences designed for BRCA1/2 mutational status and methylation of the BRCA1 promoter assessment are detailed in Tables 2, 3, and 4, respectively.

IHC Analysis

Tissue sections (4 μm thick) were cut from formalin-fixed, paraffin-embedded representative blocks of 16 of 19 MBCs and 27 of 36 non-MBC BLCs sampled and gathered in a tissue microarray. After deparaffinization according to standard procedures, all sections were subjected to heat-induced antigen retrieval in citrate buffer (pH 6.1). Antibody against BCLG (clone ab184925, Abcam, Cambridge, UK) was then applied and staining was performed with the Vectastain Elite ABC peroxidase mouse IgG kit (Vector Laboratories, Burlingame, CA), with diaminobenzidine (Dako, Santa Clara, CA) as chromogen. Semiquantitative assessment of expression was performed using a light microscope by two independent readers (P.R., G.D.) according to the following algorithm: the staining intensity in tumor cells was graded on a scale of 0 (no expression) to 3 (for highest intensity). The entire section was assessed. The percentage of positive tumor cells was calculated for each specimen, and this percentage score was multiplied by the staining intensity to obtain a final semiquantitative H score that ranged from 0 to 300. The mean H score based on scoring by the two readers was attributed to each tumor sample. The t-test was used to assess specificity of IHC staining between the two groups. Spearman's rank correlation test was used to assess the correlation between H score and BCLG expression level.

RNA Sequencing

Library preparation and paired-end (2 × 100 bp) RNA sequencing were performed on six MBCs by IntegraGen (Evry, France) using a TruSeq RNA sample preparation kit and HiSeq 2000 platform (both from Illumina, San Diego, CA), respectively. A mean of 130 million reads were obtained for each sample. RNA sequencing raw reads were mapped using TopHat version 2.0.6 (Johns Hopkins University Center for Computational Biology, Baltimore, MD; https://ccb.jhu.edu/software/tophat/index.shtml, last accessed April 9, 2018) and Bowtie version 2.0.4 (Johns Hopkins University Center for Computational Biology; http://bowtie-bio.sourceforge.net/bowtie2/index.shtml) against UCSC hg19 genome (National Center for Biotechnology Information build 37.1). Single-nucleotide variants and transcriptome quantitative analysis were performed using SAM tools version 0.1.8 and Cufflinks version 2.0.2 (Cole Trapnell, Seattle, WA; http://cole-trapnell-lab.github.io/cufflinks, last accessed April 9, 2018), respectively. Expression levels of validated mutations were determined using RNA sequencing data. Gene fusion analyses were performed using two validated tools: TopHat-fusion version 2.0.4 and deFuse version 0.615, 16, 17 (Supplemental Table S3). Gene fusion validation was performed using RT-qPCR and Sanger sequencing (primer sequences used are detailed in Table 5).

TNBC Subtyping

Gene expression levels obtained from GeneChip Human Genome U133 Plus 2.0 Array analysis were submitted as preprocessed and normalized data to the web-based subtyping tool TNBCtype for candidate TNBC samples according to the web-interface developers' instructions (http://cbc.mc.vanderbilt.edu/tnbc, last accessed April 9, 2018). Briefly, gene expression values expressed in cnv format (ASCII format file delimited by comma) were uploaded for each sample in the genome-wide TNBC gene expression matrix based on a data set of 3247 gene expression profiles from 21 breast cancers. After format checking, 18 of 19 MBC cases and 28 of 35 non-MBC BLC cases were classified into one of the six predicted TNBC subtypes based on the gene expression matrix profiles, with corresponding correlation coefficients and permutation P values. TNBC subtypes include basal-like 1 (BL1) and basal-like 2 (BL2) subtypes, immunomodulatory (IM) subtype, mesenchymal (M) subtype, mesenchymal stem-like (MSL) subtype, and luminal androgen (LAR) subtype, defined according to shared unique profiles among 587 TNBC samples. Tumors with no predominant gene expression profile were classified as unstable.18 Finally, in accordance with the refined classification of TNBCtype, the so-called TNBCtype-4,19 IM and MSL cases were reassessed to the second highest correlated centroid among BL1, BL2, M, and LAR subtypes.

Survival Analysis

Survival analysis was conducted on an extended cohort of 32 MBCs and 44 non-MBC BLCs. Differences between groups were compared by a $\chi 2$ test or Fisher's exact test for categorical variables. Disease-free survival was defined as the time elapsed between diagnosis of the primary tumor and occurrence of the first event, either recurrence, metastasis, or death. Overall survival (OS) was based on a similar definition without taking the recurrence and metastasis events into account. Patients who were still alive and those free of disease recurrence at the time of last follow-up were censored at the date of last known contact. Both OS and disease-free survival (DFS) were estimated using the Kaplan-Meier method, and groups were compared using the log-rank test. Statistical significance was set at $P < 0.05$, and analyses were performed using R version 3.0.1 statistical software (The Comprehensive R Archive Network, Vienna, Austria; http://cran.r-project.org, last accessed April 9, 2018).

Results

MBC Has a Distinct Gene Expression Profile from Non-MBC BLC

Among the studied series, two different transcriptomic groups of tumors were identified, as shown in dendro-heatmaps in Figure 1 (unsupervised analysis). The first cluster was predominantly [29 of 30 (97%)] composed of non-MBC BLCs, and the second cluster was mostly [18 of 24 (75%)] composed of MBCs ($P < 0.05$). Supervised transcriptomic data were then analyzed to precisely identify deregulated genes in these two groups and showed that 154 genes were underexpressed in MBCs compared with non-MBC BLCs and that 92 genes were overexpressed in MBCs compared with non-MBC BLCs (Supplemental Table S4). BCLG (alias BCL2L14) was the most differentially overexpressed gene in MBCs compared with non-MBC BLCs (fold change = 23) (Figure 2A). Interestingly, those non-MBC BLCs with BCLG overexpression were associated with a high TILs infiltrate (Supplemental Table S5).

A Gene Ontology study was performed to identify the biological processes in which these genes are involved. Significantly represented Gene Ontology pathways identified are listed in Supplemental Table S6 (supervised analysis). On the basis of the overexpressed genes in MBC, 110 Gene Ontology biological processes were identified with most immunity and inflammatory response–related pathways, whereas six pathways related to developmental processes resulted from the analysis based on underexpressed genes in MBC.

BCLG Overexpression in MBC Is Confirmed by RT-qPCR in the Validation Cohort

This validation analysis found that the NBCLG ranged from 0.18 to 2.82 among normal breast samples and that BCLG was overexpressed (transcript level ≥3 compared with the median NBCLG of normal tissue normalized as 1) in 78.9% of MBCs versus 42.9% of non-MBC BLCs and 40.2% of TNBCs ($P = 0.006$). Among the 41 of the 101 TNBCs that overexpressed BCLG, three were defined as atypical MBC and one was defined as MBC. BCLG expression was higher in TNBC than in the other subgroups (Figure 2B). It was therefore confirmed that BCLG overexpression is significantly more frequently found in MBC.

Analysis of overexpression of the three BCLG transcripts (Materials and Methods) in MBC revealed that the median NBCLG-L was 31.68 (range, 0.00 to 2372.84) and the median NBCLG-S was 1.11 (range, 0.00 to 47.57) in these tumors (data not shown). The long variant transcript of the gene, encoding for a 327–amino acid protein, was therefore mainly responsible for BCLG overexpression in breast tumors.

To determine whether BCLG overexpression in breast tumors was related to the epithelial or stromal component of the tumor and because of the high density of TILs in MBC, BCLG expression was assessed in epithelial cell lines and PDX tumors (Figure 2C). BCLG gene expression was null or minimal in seven nontumor cell lines. It is noteworthy that 7 of 31 tumor cell lines (22.6%) (HCC-1187, HCC-38, HCC-70, MDA-MB-468, HCC-1937, MDA-MB-415, BT474) had a median NBCLG >4. Five of these seven cell lines were derived from TNBC tumors. The highest BCLG expression was observed in the HCC-70 cell line (N = 62.7) and the HCC 1187 cell line (N = 20.8), known to belong to the IM subgroup according to Lehmann et al.18 Notably, the two ER+ cell lines (MDA-

MB-415 and BT474) that expressed higher levels of BCLG lack progesterone receptor expression (Supplemental Table S2).20 Overexpression of human BCLG expression (CT < 32) was observed in 38 of 61 PDXs (62.3%), and murine BCLG expression was observed in only 5 of 61 cases (8.1%). Equally interesting, 27 of 38 PDXs (69.2%) overexpressing human BCLG were TNBC PDXs. Therefore, it can be concluded that BCLG overexpression is related to the epithelial component of the tumor.

Finally, epithelial expression of BCLG was also confirmed by IHC studies performed on 16 MBCs and 27 non-MBC BLCs. A granular cytoplasmic BCLG staining pattern was observed in carcinomatous cells. TILs did not express BCLG (Figure 2D). The median H score in MBC was higher than in non-MBC BLCs (107.5 versus 50.0, P = 0.019) (Figure 2E). Furthermore, MBC tumors were enriched with high BCLG H score cases (H score >200) (Supplemental Table S7). BCLG transcript and protein expression levels were correlated in this series (Figure 2F).

BCLG Overerxpression in MBC Is Not Related to Copy Number Alterations

BCLG copy number localized at chromosome 12p13.2 was assessed in all samples of the initial cohort (Table 6). BCLG gains were observed in 8 of 19 (42%), including two focal amplifications, of MBCs and 25 of 36 (69%), including nine focal amplifications, of non-MBC BLCs. Conversely, BCLG losses were observed in 6 of 19 MBCs (32%) and 5 of 36 non-MBC BLCs (14%). These results therefore indicate that BCLG gene overexpression in MBC is not related to copy number alterations. Similarly, no correlation was observed between BCLG expression level and high LST or low LST status in MBCs or non-MBC BLCs (data not shown).

RNA Sequencing Identifies Putative Fusion Candidate Genes in MBC

RNA sequencing identified eight putative fusion candidate genes common to the two analysis tools in six MBCs, which were then validated by RT-qPCR and Sanger sequencing (Supplemental Table S8). These fusions were not recurrent among the 19 MBCs.

MBC Belongs to the IM Subgroup from the Original TNBC Classification and to the BL1 Subgroup in the Four Classes Refined Classification

To investigate whether MBC belongs to one of the previously defined transcriptomic TNBC subgroups, the MBC transcriptomic profile was submitted to the online tool developed by Lehmann et al.18 This analysis found that 15 of 18 MBCs belonged to the IM group versus only 3 of 28 non-MBC BLCs by using the original TNBC classification of six classes (Figures 1 and 3). In the refined TNBCtype-4 classification, 11 of 18 MBCs belonged to the BL1 group versus 6 of 28 non-MBC BLCs (P < 0.05) (Figures 1 and 3). Interestingly, the three non-MBC BLCs classified as IM in the TNBCtype classification (and as one BL1 and two BL2 in the TNBCtype-4 classification) belonged to the MBC-enriched transcriptomic cluster (Figure 1). Retrospective review of pathology specimens found that two of these tumors could be morphologically be selected as invasive breast carcinoma NST with medullary features, whereas the third could be classified as invasive breast carcinoma NST, with central acellular zone. The stromal signature defined by Lehmann et al19 did not segregate MBCs from non-MBC BLCs in our cohort (data not shown). Consequently, this study found that the

morphologically selected MBC cases belonged, at the transcriptomic level, to the IM and BL1 subgroups as defined by Lehmann et al.18, 19

MBCs Is Characterized by Frequent LOH

Notably, copy number analysis performed between MBC and non-MBC BLC found, for the first time to our knowledge, 23 recurrent loss of heterozygosity (LOH) specific to MBC and five recurrent LOH specific to non-MBC BLC ($P < 0.05$), listed in detail in Table 7 and plotted as a function of genome location in Figure 4. Recurrent gains and losses are listed in the Supplemental Table S9 and recurrent focal amplicons in Supplemental Table S10. Finally, 11 of 16 MBCs (69%) and 21 of 34 non-MBC BLCs (62%) had high LST status, reflecting BRCA1/2 inactivation (no significant difference) (Supplemental Table S11).

MBC Has a Better OS and DFS than Non-MBC BLC

All patients in the extended cohort of 32 MBCs and 44 non-MBC BLCs were women between the ages of 27 and 89 years, with a mean age of 53 years. Median clinical follow-up was 101 months (range, 14 to 237 months). Four patients (12.5%) in the MBC group and 13 patients (29.5%) in the non-MBC BLC group died during follow-up. On univariate analysis, MBC, TIL-rich tumors, and N0 cases had a better OS and DFS. On multivariate analysis, MBC subtype and TILs were correlated with a better OS and DFS ($P = 0.02$ for both criteria).

Discussion

This study found that MBC has a specific transcriptomic pattern compared with non-MBC BLC and overexpresses more frequently the long isoform of the BCLG gene than other subtypes of breast cancer. BCLG overexpression was confirmed at the protein level to be significantly associated with MBC. Moreover, this study found that MBC belonged to the IM subgroup in the six-class system of Lehmann et al18 and to the BL1 subgroup in the four-class system,19 respectively. Finally, this study refined the genomic landscape of MBC, harboring more LOH than non-MBC BLC.

The gene expression analysis performed in our series emphasized as expected up-regulation of inflammatory and immune responses pathways in MBC, as previously described in the pioneer study by Bertucci et al.2 In addition to that, MBC preferentially belonged to the IM TNBC subtype according to the six groups originally defined by Lehmann et al.18 The latter previously reported that immune signaling genes overexpressed in the IM subtype overlapped with the MBC gene signature as established by Bertucci et al,2 suggesting that IM could be at least partially represented by MBC.18 Bareche et al21 reviewed a posteriori the morphology from the TCGA and METABRIC data sets and found an enrichment (15%) of MBC in the IM subgroup. Teschendorff et al22 found that MBC belonged to an ER-negative gene expression cluster characterized by overrepresentation of genes involved in cell cycle/proliferation and immune response. The favorable outcome of the IM subtype is likely linked to overexpression of immune pathways. Moreover, it is now broadly accepted that TILs are usually associated with a better prognosis in ER-negative cancer.23 The better outcome of MBC was indeed related to a high TILs infiltrate when compared with non-MBC BLC in our series. Our study found that MBC, selected morphologically, clearly belong to the IM transcriptomic category. Interestingly, it has been suggested that IM may specifically respond to poly (ADP-ribose) polymerase inhibitors and cisplatin-based therapy.24 Vinayak et al25 found that the presence of both

stromal and intratumoral TILs specifically promoted the response to platinum- and poly (ADP-ribose) polymerase inhibitor–based neoadjuvant chemotherapy in IM-TNBC (PrECOG 0105).

Using the refined classification by Lehman et al19 based on only four groups, MBC predominantly pertained to the BL1 subgroup, which is characterized by aberrant DNA signaling and repair functions.18 This finding is in line with the well-documented high prevalence of BRCAness feature in MBC, confirmed in this study through the LST status.

Taken together, our MBC transcriptomic data refined the position of this entity in the taxonomy of TNBC and confirmed the importance of considering both the involvement of T-cell regulation and DNA repair deregulation pathways for further therapeutic approaches to this tumor type. In addition, BRCAness traits in MBC support that, from a biological point of view, MBC is a good candidate to respond to homologous recombination deficiency targeting drugs and immunotherapy. However, given the intrinsic good prognosis of typical forms of MBC, it may be of interest to integrate morphologic and biological specification of the tumor in the clinical management of MBC. It may still be hypothesized that in advanced disease MBC may benefit from the same therapeutic strategies as those developed in TNBC in general.

Overexpression of the long isoform of BCLG was found to be one of the major molecular characteristics of epithelial cells in most MBCs but in less than half of the non-MBC BLCs. Interestingly, BCLG overexpression was not determined by gene amplification. It is well known that gene expression is associated with copy number changes in breast cancer only in a limited proportion of cases.26 Of note, this study described a high prevalence of LOH in MBC compared with non-MBC BLC; however, BCLG was not included in a recurrent LOH region in MBC. Thus, it can be hypothesized that epigenetic dysregulation may be implicated. Indeed, DNA methylation alterations have been described as associated with BCLG variations of expression in different pathological contexts.27, 28 DNA hypomethylation, associated with gene overexpression, is largely prevalent in cancer, especially in TNBC of good prognosis.29, 30, 31 Thus, DNA methylation alterations may participate, at least partially, to BCLG overexpression in MBC. It has been previously reported that BCLG is down-regulated in breast cancer, regardless of histological or molecular subtype.32 This new observation emphasizes the significant association of BCLG overexpression and MBC. BCLG has been extensively studied in terms of its role as a proapoptotic gene, although antiapoptotic functions of BCLG have been also reported in cancer cell lines.33 Notably, BCLG mediates apoptosis under the control of several factors, such as FAU and maternal embryonic leucine zipper kinase (MELK), in breast cancer cell lines.34 Lin et al34 found that the MELK oncoprotein specifically inhibited BCLG-L–induced apoptosis in breast cancer cell lines. Interestingly, Nakamura et al35 found that the ubiquitin-like protein monoclonal nonspecific suppressor factor β–BCLG complex enhanced apoptosis and inhibited IL-4 production via ERK phosphorylation in T cells. Moreover, transfection studies found that BCLG-L enhanced apoptosis in CD4+ T cells from healthy subjects.36 Altogether, these findings suggest that BCLG-L may have a proapoptotic role in breast cancers rich in TILs, such as MBC or TILs-rich non-MBC BLC. Furthermore, whether BCLG plays a role in increasing the TILs density remains to be determined. Lastly, BCLG is a target gene for TP53, known to be mutated in up to 100% of MBC.4 It would be particularly useful to determine whether BCLG overexpression in MBC is a compensatory mechanism for TP53 dysfunction.

In conclusion, this study provides an in-depth molecular portrait of MBC. MBC overexpresses BCLG more frequently than non-MBC BLC. Non-MBC BLC overexpressing BCLG is TILs enriched. These data suggest that MBC may represent the end of a spectrum of BLC with enrichment in immune infiltrate together with an increased BCLG overexpression. Furthermore, our study found that MBC belongs not only to the IM subgroup from the six categories defined by Lehmann et al18 but also to the BL1 subgroup from the four group classification of Lehmann et al19 based on epithelial carcinomatous cells characteristics only. This finding led us to conclude that immune pathways activation together with DNA repair alterations importantly define MBC in regard of non-MBC BLC. TILs activation mechanisms underlying MBC biology should be considered as the main areas of investigation in this specific entity to more clearly understand its better prognosis and propose more appropriate therapeutic approaches.

Supplemental Data

Supplemental material for this article can be found at https://doi.org/10.1016/j.ajpath.2018.06.021.

Supported by the Grand Prix Ruban Rose 2012 (A.V.-S.) and in part by a grant from the Mayent-Rothschild Foundation (C.M.). Disclosures: A patent based on the data presented in this report is pending (US Patent application US20170260588A1; T.P. and M.-H.S. are the named inventors). The patent is currently licensed to Myriad Genetics.

References

1 L. Pedersen, K. Zedeler, S. Holck, H.T. Mouridsen Medullary carcinoma of the breast. Prevalence and prognostic importance of classical risk factors in breast cancer Eur J Cncer, 31A (1995), pp. 2289-2295

2 F. Bertucci, P. Finetti, N. Cervera, E. Charafe-Jauffret, E. Mamessier, J. Adélaïde, S. Debono, G. Houvenaeghel, D. Maraninchi, P. Viens, C. Charpin, J. Jacquemier, D. Birnbaum Gene expression profiling shows medullary breast cancer is a subgroup of basal breast cancers Cancer Res, 66 (2006), pp. 4636-4644

3 A. Vincent-Salomon, N. Gruel, C. Lucchesi, G. MacGrogan, R. Dendale, B. Sigal-Zafrani, M. Longy, V. Raynal, G. Pierron, I. de Mascarel, C. Taris, D. Stoppa-Lyonnet, J.Y. Pierga, R. Salmon, X. Sastre-Garau, A. Fourquet, O. Delattre, P. de Cremoux, A. Aurias Identification of typical medullary breast carcinoma as a genomic sub-group of basal-like carcinomas, a heterogeneous new molecular entity Breast Cancer Res, 9 (2007), p. R24

4 P. de Cremoux, A.V. Salomon, S. Liva, R. Dendale, B. Bouchind'homme, E. Martin, X. Sastre-Garau, H. Magdalenat, A. Fourquet, T. Soussi p53 mutation as a genetic trait of typical medullary breast carcinoma J Natl Cancer Inst, 91 (1999), pp. 641-643

5 J. Huober, S. Gelber, A. Goldhirsch, A.S. Coates, G. Viale, C. Öhlschlegel, K.N. Price, R.D. Gelber, M.M. Regan, B. Thürlimann Prognosis of medullary breast cancer: analysis of 13 International Breast Cancer Study Group (IBCSG) trials Ann Oncol, 23 (2012), pp. 2843-

6 R.L. Ridolfi, P.P. Rosen, A. Port, D. Kinne, V. Miké Medullary carcinoma of the breast: a clinicopathologic study with 10 year follow-up Cancer, 40 (1977), pp. 1365-1385

7 R. Salgado, C. Denkert, S. Demaria, N. Sirtaine, F. Klauschen, G. Prunieri, S. Wienert, G. Van den Eynden, F.L. Baehner, F. Penault-Llorca, E.A. Perez, E.A. Thompson, W.F. Symmans, A.L. Richardson, J. Brock, C. Criscitiello, H. Bailey, M. Ignitiadis, G. Floris, J. Sparano, Z. Kos, T. Nielsen, D.L. Rimm, K.H. Allison, J.S. Reis-Filho, S. Loibl, C. Sotiriou, G. Viale, S. Badve, S. Adams, K. Willard-Gallo, S. Loi The evaluation of tumor-infiltrating lymphocytes (TILs) in breast cancer: recommendation by an International TILs Working Group 2014 Ann Oncol, 26 (2015), pp. 259-271

8 P. Chomczynski, N. Sacchi Single-step method of RNA isolation by acid guanidinium thiocyanate-phenol-chloroform extraction Anal Biochem, 162 (1987), pp. 156-159

9 H. Mi, X. Huang, A. Muruganujan, H. Tang, C. Mills, D. Kang, P.D. Thomas PANTHER version 11: expanded annotation data from Gene Ontology and Reactome pathways, and data analysis tool enhancements Nucleic Acids Res, 45 (2017), pp. D183-D189

10 I. Bieche, P. Onody, I. Laurendeau, M. Olivi, D. Vidaud, R. Lidereau, M. Vidaud Real-time reverse transcription-PCR assay for future management of ERBB2-based clinical applications Clin Chem, 45 (1999), pp. 1148-1156

11 I. Bieche, B. Parfait, V. Le Doussal, M. Olivi, M.C. Rio, R. Lidereau, M. Vidaud Identification of CGA as a novel estrogen receptor-responsive gene in breast cancer: an outstanding candidate marker to predict the response to endocrine therapy Cancer Res, 61 (2001), pp. 1652-1658

12 T. Popova, E. Manié, D. Stoppa-Lyonnet, G. Rigaill, E. Barillot, M.H. Stern Genome Alteration Print (GAP): a tool to visualize and mine complex cancer genomic profiles obtained by SNP arrays Genome Biol, 10 (2009), p. R128

13 T. Popova, E. Manié, G. Rieunier, V. Caux-Moncoutier, C. Tirapo, T. Dubois, O. Delattre, B. Sigal-Zafrani, M. Bollet, M. Longy, C. Houdayer, X. Sastre-Garau, A. Vincent-Salomon, D. Stoppa-Lyonnet, M.H. Stern Ploidy and large-scale genomic instability consistently identify basal-like breast carcinomas with BRCA1/2 inactivation Cancer Res, 72 (2012), pp. 5454-5462

14 E. Manié, A. Vincent-Salomon, J. Lehmann-Che, G. Pierron, E. Turpin, M. Warcoin, N. Gruel, I. Lebigot, X. Sastre-Garau, R. Lidereau, A. Remenieras, J. Feunteun, O. Delattre, H. de Thé, D. Stoppa-Lyonnet, M.H. Stern High frequency of TP53 mutation in BRCA1 and sporadic basal-LIKE carcinomas but not in BRCA1 luminal breast tumors Cancer Res, 69 (2009), pp. 663-671

15 D. Kim, S.L. Salzberg TopHat-Fusion: an algorithm for discovery of novel fusion transcripts Genome Biol, 12 (2011), p. R72

16 A. McPherson, F. Hormozdiari, A. Zayed, R. Giuliany, G. Ha, M.G. Sun, M. Griffith, A. Heravi Moussavi, J. Senz, N. Melnyk, M. Pacheco, M.A. Marra, M. Hirst, T.O. Nielsen, S.C. Sahinalp, D. Huntsman, S.P. Shah deFuse: an algorithm for gene fusion discovery in tumor RNA-Seq data PLoS Comput Biol, 7 (2011), p. e1001138

17 C. Trapnell, L. Pachter, S.L. Salzberg TopHat: discovering splice junctions with RNA-Seq Bioinformatics, 25 (2009), pp. 1105-1111

18 B.D. Lehmann, J.A. Bauer, X. Chen, M.E. Sanders, A.B. Chakravarthy, Y. Shyr, J.A. Pietenpol Identification of human triple-negative breast cancer subtypes and preclinical models for selection of targeted therapies J Clin Invest, 121 (2011), pp. 2750-2767

19 B.D. Lehmann, B. Jovanović, X. Chen, M.V. Estrada, K.N. Johnson, Y. Shyr, H.L. Moses, M.E. Sanders, J.A. Pietenpol Refinement of triple-negative breast cancer molecular subtypes: implications for neoadjuvant chemotherapy selection PLoS One, 11 (2016), p. e0157368

20 G. Jiang, S. Zhang, A. Yazdanparast, M. Li, A.V. Pawar, W. Liu, S.M. Inavolu, L. Cheng Comprehensive comparison of molecular portraits between cell lines and tumors in breast cancer BMC Genomics, 17 Suppl 7 (2016), p. 525

21 Y. Bareche, D. Venet, M. Ignatiadis, P. Aftimos, M. Piccart, F. Rothe, C. Sotiriou Unravelling triple-negative breast cancer molecular heterogeneity using an integrative multiomic analysis Ann Oncol, 29 (2018), pp. 895-902

22 A.E. Teschendorff, A. Miremadi, S.E. Pinder, I.O. Ellis, C. Caldas An immune response gene expression module identifies a good prognosis subtype in estrogen receptor negative breast cancer Genome Biol, 8 (2007), p. R157

23 E.M. Ibrahim, M.E. Al-Foheidi, M.M. Al-Mansour, G.A. Kazkaz The prognostic value of tumor-infiltrating lymphocytes in triple-negative breast cancer: a meta-analysis Breast Cancer Res Treat, 148 (2014), pp. 467-476

24 V.G. Abramson, B.D. Lehmann, T.J. Ballinger, J.A. Pietenpol Subtyping of triple-negative breast cancer: implications for therapy Cancer, 121 (2015), pp. 8-16

25 S. Vinayak, R.J. Gray, S. Adams, K.C. Jensen, J. Manola, A. Afghahi, L.J. Goldstein, J.M. Ford, S.S. Badve, M.L. Telli Association of increased tumor-infiltrating lymphocytes (TILs) with immunomodulatory (IM) triple-negative breast cancer (TNBC) subtype and response to neoadjuvant platinum-based therapy in PrECOG0105 J Clin Oncol, 32 (2014) 15_suppl, 1000-1000

26 K. Chin, S. DeVries, J. Fridlyand, P.T. Spellman, R. Roydasgupta, W.L. Kuo, A. Lapuk, R.M. Neve, Z. Qian, T. Ryder, F. Chen, H. Feiler, T. Tokuyasu, C. Kingsley, S. Dairkee, Z. Meng, K. Chew, D. Pinkel, A. Jain, B.M. Ljung, L. Esserman, D.G. Albertson, F.M. Waldman, J.M. Gray Genomic and transcriptional aberrations linked to breast cancer pathophysiologies Cancer Cell, 10 (2006), pp. 529-541

27 D. Balasubramanian, B. Akhtar-Zaidi, L. Song, C.F. Bartels, M. Veigl, L. Beard, L. Myeroff, K. Guda, J. Lutterbaugh, J. Willis, G.E. Crawford, S.D. Markowitz, P.C. Scacheri H3K4me3 inversely correlates with DNA methylation at a large class of non-CpG-island-containing start sites Genome Med, 4 (2012), p. 47

28 P. Coit, M. Jeffries, N. Altorok, M.G. Dozmorov, K.A. Koelsch, J.D. Wren, J.T. Merrill, McCuneWJ, A.H. Sawalha Genome-wide DNA methylation study suggests epigenetic accessibility and transcriptional poising of interferon-regulated genes in naïve CD4+ T cells from lupus patients J Autoimmun, 47 (2013), pp. 78-84

29 A.H. Ting, K.M. McGarvey, S.B. Baylin The cancer epigenome – components and functional correlates Genes Dev, 20 (2006), pp. 3215-3231

30 K. Jackson, M.C. Yu, K. Arakawa, E. Fiala, B. Youri, H. Fiegl, E. Müller-Holzner, M. Wolschwendter, M. Ehrlich DNA hypomethylation is prevalent even in low-grade breast cancers Cancer Biol Ther, 3 (2004), pp. 1225-1231

31 C. Stirzaker, E. Zotenko, J.Z. Song, W. Qu, S.N. Nair, W.J. Locke, A. Stone, N.J. Armstrong, M.D. Robinson, A. Dobrovic, K.A. Avery-Kiejda, K.M. Peters, J.D. French, S. Stein, D.J. Korbie,

M. Trau, J.F. Forbes, R.J. Scott, M.A. Brown, G.D. Francis, S.J. Clark Methylome sequencing in triple-negative breast cancer reveals distinct methylation clusters with prognostic value Nat Commun, 6 (2015), p. 5899

32 M.R. Pickard, A.R. Green, I.O. Ellis, C. Caldas, V.L. Hedge, M. Mourtada-Maarabouni, G.T. Williams Dysregulated expression of Fau and MELK is associated with poor prognosis in breast cancer Breast Cancer Res, 11 (2009), p. R60

33 M.R. Pickard, M. Mourtada-Maarabouni, G.T. Williams Candidate tumour suppressor Fau regulates apoptosis in human cells: an essential role for Bcl-G Biochim Biophys Acta, 1812 (2011), pp. 1146-1153

34 M.-L. Lin, J.-H. Park, T. Nishidate, Y. Nakamura, T. Katagiri Involvement of maternal embryonic leucine zipper kinase (MELK) in mammary carcinogenesis through interaction with Bcl-G, a pro-apoptotic member of the Bcl-2 family Breast Cancer Res, 9 (2007), p. R17

35 M. Nakamura, M. Nakagawa, J. Watanabe Ubiquitin-like protein MNSFβ negatively regulates T cell function and survival Immunol Invest, 44 (2015), pp. 1-12 CrossRefView Record in Scopus 36 N. Luo, Y. Wu, Y. Chen, Z. Yang, S. Guo, L. Fei, D. Zhou, C. Yang, S. Wu, B. Ni, F. Hao, Y. Wu Upregulated BclG(L) expression enhances apoptosis of peripheral blood CD4+ T lymphocytes in patients with systemic lupus erythematosus Clin Immunol, 132 (2009), pp. 349-361

Tables

Table 1. Nucleotide Sequences of the Quantitative RT-PCR Primers for *BCLG*

Transcript	Forward	Reverse
TBP	5′-TGCACAGGAGCCAAGAGTGAA-3′	5′-CACATCACAGCTCCCCACCA-3′
BCLG human	5′-GCCAGCAGTGGTCCAGGTGTCT-3′	5′-CTACTCGGTTGGCAATGGAAATGA-3′
BCLG long	5′-CACGTGCCTGTAGCTTCAAGTTC-3′	5′-AAGCCTTATCTTTCTTCAGCTTTCTT-3′
BCLG short	5′-CACGTGCCTGTAGCTTCAAGTTCT-3′	5′-GGGATGAAGGCAGTGTCCTTTCT-3′
BCLG murin	5′-AGCACTGGCCCAGGTCTCTGA-3′	5′-CAGCCACTCTGTTGGCAATACAAG-3′

Table 2. Nucleotide Sequences of the PCR Primers for *BRCA1* Mutational Status Assessment

***BRCA1*amplicons**	**Screened region**	**Forward**	**Reverse**
02speA, 02speB	UTR-5′-170–IVS02+127	5′-AATAAAGGACGTTGTCATTAGTTCT-3′	5′-AGCAATTACAATAGCCTAATCTTAC-3′
03eA, 03eB	IVS02-164–IVS03+201	5′-TTCCTGACACAGCAGACATTT-3′	5′-ATGTCAAAACTTTACCAGGAAC-3′
05eA, 05eB	IVS04-128–IVS05+110	5′-GCCATTACTTTTTAAATGGCTC-3′	5′-TTATAAATTTTTCTGATGAATGGTT-3′
06eA, 06eB	IVS05-121–IVS06+122	5′-AGAGGTTTTCTACTGTTGCTG-3′	5′-CAGAACTAAAATTAACCTAGACT-3′
07eA, 07eB	IVS06-125–IVS07+114	5′-GGTAACCTTAATGCATTGTCTT-3′	5′-AAGGCAGGAGGACTGCTTCT-3′
08eA, 08eB	IVS07-154–IVS08+108	5′-TGTGTAAATTCCTGGGCATT-3′	5′-CAAAGCTGCCTACCACAAATA-3′
09eA, 09eB	IVS08-121–IVS09+132	5′-CCACAGTAGATGCTCAGTAAA-3′	5′-AACAAACTGCACATACATCCC-3′
10eA, 10eB	IVS09-121–IVS10+109	5′-CTAAATAAGATTGGTCAGCTTTCT-3′	5′-TTTTGTGGGTTGTAAAGGTCC-3′
11-01eA, 11-01eB	IVS10-125–c.1097	5′-GTTTATGAGGTTAGTTTCTCTAA-3′	5′-TCTCTAGGATTCTCTGAGCAT-3′

*BRCA1*amplicons	Screened region	Forward	Reverse
11-02eA, 11-02eB	c.942–c.1463	5′-AAGGAGCCAACATAACAGATG-3′	5′-GTAACAAATGCTCCTATAATTAG-3′
11-03eA, 11-03eB	c.1326–c.1850	5′-TAAAAGTGAAAGAGTTCACTCC-3′	5′-GTAGAAGACTTCCTCCTCAG-3′
11-04eA, 11-04eB	c.1702–c.2222	5′-CCTAACCCAATAGAATCACTC-3′	5′-GACACTTTAACTGTTTCTAGTTT-3′
11-05eA, 11-05eB	c.2084–c.2600	5′-ATACTTTCCCAGAGCTGAAGT-3′	5′-TGGCGCTTTGAAACCTTGAAT-3′
11-06eA, 11-06eB	c.2440–c.2959	5′-CTAATTCATGGTTGTTCCAAAG-3′	5′-TGATGGGAAAAAGTGGTGGTA-3′
11-07eA, 11-07eB	c.2799–c.3238	5′-TCAGAAAGATAAGCCAGTTGAT-3′	5′-ATTTTGGCCCTCTGTTTCTAC-3′
11-08eA, 11-08eB	c.3077–c.3629	5′-TTAGCCGTAATAACATTAGAGAA-3′	5′-TCTAATTTCTTGGCCCCTCTT-3′
11-09eA, 11-09eB	c.3468–c.3924	5′-TGGTGAAATAAAGGAAGATACTA-3′	5′-TGCAGTCAAGTCTTCCAATTC-3′
11-10eA, 11-10eB	c.3789–IVS11+127	5′-GAAGAATAGCTTAAATGACTGC-3′	5′-TTCAAGTTTAAGAAGCAGTTCC-3′
12eA, 12eB	IVS11-110–IVS12+109	5′-TGTGTGACATGAAAGTAAATCC-3′	5′-CCATTAATTCAAAGAGATGATGT-3′
13eA, 13eB	IVS12-123–IVS13+110	5′-TTGTAGTTCCATACTAGGTGAT-3′	5′-CTGAGCAAGGATCATAAAATGT-3′
14eA, 14eB	IVS13-137–IVS14+112	5′-TCTGCCTGATATACTTGTTTAAA-3′	5′-AATGCCTGTATGCAAAAAACTG-3′
15eA, 15eB	IVS14-122–IVS15+134	5′-TGCCAGTCATTTCTGATCTCT-3′	5′-GTGGGCTTAATTAAGTATAACA-3′
16eA, 16eB	IVS15-122–IVS16+116	5′-ATTCATGTACCCATTTTTCTCTT-3′	5′-GTGATTGTTTTCTAGATTTCTTC-3′
17eA, 17eB	IVS16-131–IVS17+133	5′-ATAGTTCCAGGACACGTGTA-3′	5′-CGATCTCCTAATCTCGTG-3′
18eA, 18eB	IVS17-115–IVS18+107	5′-ATAAATCCAGATTGATCTTGG-3′	5′-GTAACTCAGACTCAGCATCA-3′

***BRCA1*amplicons**	**Screened region**	**Forward**	**Reverse**
19eA, 19eB	IVS18-119–IVS19+106	5′-AAGGACCTCTCCTCTGTCAT-3′	5′-TGTGCATTGTTAAGGAAAGTG-3′
20eA, 20eB	IVS19-205–IVS20+151	5′-ATGAGGTTTCACCATGTTGGT-3′	5′-GAAGAGTGAAAAAAGAACCTGT-3′
21eA, 21eB	IVS20-116–IVS21+113	5′-AAGAAAAGCTCTTCCTTTTTGAA-3′	5′-TCTAGAACATTTCAGCAATCTG-3′
22eA, 22eB	IVS21-183–IVS22+174	5′-GTGGCAAATTGACTTAAAATCC-3′	5′-CAGTTCTCAAATCCTTACCCA-3′
23eA, 23eB	IVS22-229–IVS23+198	5′-AGGGGTGGTGGTACGTGTCT-3′	5′-CCATGGAAACAGTTCATGTATT-3′
24eA, 24eB	IVS23-120–UTR-3′+108	5′-TTAGCTTCTACCTCATTAATCC-3′	5′-AGGACAGTAGAAGGACTGA-3′

Table 3. Nucleotide Sequences of the PCR Primers for *BRCA2* Mutational Status Assessment

***BRCA2*amplicons**	**Screened region**	**Forward**	**Reverse**
	UTR-5′-156–IVS02+119	5′-AGGAGATGGGACTGAATTAGA-3′	5′-CACATAAGGAACAGTTTATGG-3′
03eA 03eB	IVS02-118–IVS03+123	5′-CAAAAGTAATCCATAGTCAAGAT-3′	5′-AGAGGCCAGAGAGACTGATT-3′
04eA 04eB	IVS03-121–IVS04+120	5′-AACTCCCTATACATTCTCATTC-3′	5′-AGATCTTCTACCAGGCTCTTA-3′
05eA 05eB	IVS04-121–Exon_6 (c.501)	5′-AATATCTAAAAGTAGTATTCCAAC-3′	5′-TGTATGAAACAAACTCCCAC-3′
06eA 06eB	Exon_5 (c.447)–IVS06+118	5′-ACATGTAACACCACAAAGAGAT-3′	5′-ATTGCCTGTATGAGGCAGAAT-3′
07eA 07eB	IVS06-119–IVS07+122	5′-ATTCTGCCTCATACAGGCAAT-3′	5′-CACACTTATCAAAGACATTATCT-3′
08eA 08eB	IVS07-114–IVS08+124	5′-TGTTTCAAATGTGTCATGTAATC-3′	5′-GACTTTCTCAAAGGCTTAGATA-3′
09eA 09eB	IVS08-121–IVS09+114	5′-GACCTAGGTTGATTGCAGATA-3′	5′-AGAGGTTGCGGTAAACCGAG-3′

*BRCA2*amplicons	Screened region	Forward	Reverse
10-01eA 10-01eB	IVS09-120–c.1135	5′-TACTGATATGTAATATTTAGCACA-3′	5′-CACTCTCAAAGGGCTTCTGA-3′
10-02eA 10-02eB	c.996–c.1457	5′-TTTCCATGAAGCAAACGCTGA-3′	5′-TGCTTTACTGCAAGAATGCAG-3′
10-03eA 10-03eB	c.1320–c.1749	5′-TACTTCAGAGAATTCTTTGCCA-3′	5′-CAAAGTGGATATTAAACCTGCA-3′
10-04eA 10-04eB	c.1610–IVS10+126	5′-AAAGTGGACTGGAAATACATAC-3′	5′-GTATACAGATGATGCCTAAGAT-3′
11-01ieA 11-01ieB	IVS10-97–c.2226	5′-ACTGTGCCCAAACACTAC-3′	5′-TTGTACTGGGTGACATGC-3′
11-01eA 11-01eB	c.2040–c.2333	5′-AGTAATCTCTCAGGATCTTGAT-3′	5′-ACATCCTTGGAAGTAGGAGTT-3′
11-02eA 11-02eB	c.2186–c.2715	5′-TAAAAGAAGAGGTCTTGGCTG-3′	5′-ATTTCCTAAAGCAAGATTATTCC-3′
11-03eA 11-03eB	c.2552–c.3081	5′-TCAACCAAAACACAAATCTAAGA-3′	5′-GCTCTTCTTAATGTTATGTTCAG-3′
11-04eA 11-04eB	c.2918–c.3445	5′-CGGACATCTCCTTGAATATAG-3′	5′-TCTGGTTTTCAGGCACTTCAA-3′
11-05eA 11-05eB	c.3306–c.3814	5′-TTTAACACCTAGCCAAAAGGC-3′	5′-TTGAAACAACAGAATCATGAC-3′
11-06eA 11-06eB	c.3671–c.4199	5′-GCACAAAACTGAATGTTTCTAC-3′	5′-TGACATGCTTCTTGAGCTTTC-3′
11-07eA 11-07eB	c.4061–c.4584	5′-CGGACTTGCTATTTACTGATC-3′	5′-GCTAGCTGTATGAAAACCCAA-3′
11-08eA 11-08eB	c.4443–c.4969	5′-GGAAACAGACATAGTTAAACAC-3′	5′-TTGTGTAACAAGTTGCAGGAC-3′
11-09eA 11-09eB	c.4834–c.5376	5′-CCACCTAAGCTCTTAAGTGAT-3′	5′-GGATATTACTTTGGAAAAACTAG-3′
11-10eA 11-10eB	c.5209–c.5739	5′-GATACTTATTTAAGTAACAGTAGC-3′	5′-ACATTCATCATTATCTAGAGAG-3′
11-11eA 11-11eB	c.5599–c.6127	5′-ACAGACAGTTTCAGTAAAGTAA-3′	5′-TTTGGGATATTAAATGTTCTGG-3′

*BRCA2*amplicons	Screened region	Forward	Reverse
11-12eA 11-12eB	c.5985–c.6512	5′-CGCAAGACAAGTGTTTTCTGA-3′	5′-ACTTTGGTTCCTAATACCAACT-3′
11-13eA 11-13eB	c.6349–c.6832	5′-TGTGTAAACTCAGAAATGGAAAA-3′	5′-TAAGGGGCTCTCCTCTTCTT-3′
11-14eA 11-14eB	c.6668–IVS11+136	5′-TTGAAACAGAAGCAGTAGAAATT-3′	5′-TCCCCCAAACTGACTACACA-3′
12eA 12eB	IVS11-141–IVS12+139	5′-TAGGTCACTATTTGTTGTAAGTA-3′	5′-TAAAGAGGTCCTTGATTAGGC-3′
13eA 13eB	IVS12-121–IVS13+119	5′-CTGTTACATTCACTGAAAATTG-3′	5′-TAAAACGGGAAGTGTTAACTTC-3′
14-01eA 14-01eB	IVS13-120–c.7207	5′-ACAAAACAGTTACCAGAATAGTA-3′	5′-TTGGTCTGCCTGTAGTAATCA-3′
14-02eA 14-02eB	c.7133–IVS14+16	5′-CAGGACATCCATTTTATCAAGT-3′	5′-AATTGTCATACAATACCTAAAGG-3′
14-03eA 14-03eB	c.7313–IVS14+153	5′-ATGGACATGGCTCTGATGATA-3′	5′-TTAAACCTAATCTTTGGATTTAGA-3′
15eA 15eB	IVS14-139–IVS15+120	5′-TGAACTCCCGACCTCAGAT-3′	5′-ATTCATCCATTCCTGCACTA-3′
16eA 16eB	IVS15-138–IVS16+144	5′-TGTTTTTGTAGTGAAGATTCTAG-3′	5′-TGCTTAACCATAATGCACTTAAAA-3′
17eA 17eB	IVS16-122–IVS17+119	5′-GAACTCATAAAAACTTAATGATCT-3′	5′-GATGGCAACTGTCACTGACAA-3′
18-01eA 18-01eB	IVS17-150–c.8222	5′-GAAACAATATATTCCTAGCTACA-3′	5′-TTTAAGACAGCTAAGAGGGGA-3′
18-02eA 18-02eB	c.8071–IVS18+215	5′-TCTGACATAATTTCATTGAGCG-3′	5′-TGGAAATGCATTATTTAAGCTCA-3′
19-01eA 19-01eB	IVS18-127–c.8467	5′-CTTCCTAAGACTTTTTAAAGTGA-3′	5′-GAATAATTACATCAACACAACCA-3′
19-02eA 19-02eB	c.8332-24–IVS19+131	5′-CAATATATTTATTAATTTGTCCAG-3′	5′-CTGCAGTGAACCAAGATCAC-3′

***BRCA2*amplicons**	**Screened region**	**Forward**	**Reverse**
20eA 20eB	IVS19-118–IVS20+120	5′-TAATCTCAGCCTCCCAAAGTT-3′	5′-TAAAGTCAATTTACTACTCAA-3′
21eA 21eB	IVS20-121–IVS21+120	5′-GCAGTTATATAGTTTCTTATCTTTA-3′	5′-ATCCCTTTTGAGAAATGCAGC-3′
22eA 22eB	IVS21-119–IVS22+122	5′-ACACCCTTAAGATGAGCTCTA-3′	5′-GTGGATTTTGCTTCTCTGATAT-3′
23eA 23eB	IVS22-120–exon_24 (c.9152)	5′-AAATCCACTACTAATGCCCAC-3′	5′-GGCTGGTAAATCTGAAATAAAAT-3′
24-01eA 24-01eB	Exon_23 (c.9094) – IVS24+17	5′-AAAACTCAGTATCAACAACTACC-3′	5′-ACTATATTGTGCATTACCTGTTT-3′
24-02eA 24-02eB	c.9118-7–IVS24+141	5′-TCTGTAGGTTTCAGATGAAATTTT-3′	5′-GAGGTTCAAAGAGGCTTACTT-3′
25eA 25eB	IVS24-82–IVS25+116	5′-CATATTAGAGTTTCCTTTCTTGC-3′	5′-CTTTACCTCACATACTACCTCA-3′
26eA 26eB	IVS25-120–IVS26+144	5′-AGGGTTTTTCATTCTTTTTTGGT-3′	5′-AACTATACTTACAGGAGCCAC-3′
27-01eA 27-01eB	IVS26-117–c.10007	5′-GAGGGAGACTGTGTGTAATAT-3′	5′-CTTTCCAAAAGAGAAATTTCATTG-3′
27-02eA 27-02eB	c.9877–UTR-3′+134	5′-GCTGCACAGAAGGCATTTCA-3′	5′-CTTTGCTCATTGTGCAACATAA-3′

Table 4. Nucleotide Sequences of the *BRCA1* Promoter Methylation Status Assessment

***BRCA1* promoter status**	**Forward**	**Reverse**
BRCA1 promoter, methylated reaction	5′-TTGGTTTTTGTGGTAATGGAAAAGTGT-3′	5′-CAAAAAATCTCAACAAACTCACACCA-3′
BRCA1 promoter, unmethylated reaction	5′-TCGTGGTAACGGAAAAGCGC-3′	5′-AAATCTCAACGAACTCACGCCG-3′

Table 5. Nucleotide Sequences of the Gene Fusion Validation Study

Transcript	Forward	Reverse
KIAA1467-ETV6	5′-CCAGCCTTCACCACCTTTAC-3′	5′-GCGAAAGTCCTCTTTGGTCA-3′
STAG1-CEP70	5′-CCTCTCCAGCAATGATTACTTC-3′	5′-CAATGCGATCTTCTTCCTCCT-3′
CCDC132-AKAP9	5′-TTTCAAGAATTACCATAGGAACACG-3′	5′-TTGAGCTGCTCTATTTCTTCTTCTC-3′
TNPO2-SHCBP1	5′-CGTAGCACTGGATCTGCTCA-3′	5′-CCATGGATATCTTGGGAATG-3′
IFT140-AATF	5′-AGACCCCTGCGGAGACTTTGT-3′	5′-TTTTTGTGGATTTTGCTTCG-3′
MAP3K11-RELA	5′-CCAGAATGGGAGGAGAAGGT-3′	5′-GAGCCTGGGGCAGGACTT-3′
ZFAND3-RNF8	5′-CCGAGCACCATGGGAGAC-3′	5′-CTCTGTTCAGCCAAACACCA-3′
TMEM123-MMP20	5′-CAGGTGCTAGCGCTGCTG-3′	5′-TCCACTTCTCAGCATTGTCG-3′
LOH12CR1-ETV6	5′-CAACAAATGCCAAATTGGAG-3′	5′-CGAGTCTTCCTCCATCCTGA-3′
CTSC-RAB38	5′-CAAACCTGCACCACTGACTG-3′	5′-CACTTTGCCACTGCTTCAAA-3′

Table 6. Copy Number Alterations of *BCLG* Chromosomal Region (12p13.2) in Medullary Breast Carcinoma (MBC) and Non-MBC Basal-Like Carcinoma (BLC)

Genomic status	MBC, *n* (%)	Non-MBC BLC, *n* (%)
Gain	8 (42)	25 (69)
Focal amplification	2 (11)	9 (25)
Loss	6 (32)	5 (14)

n = 19 MBC; *n* = 36 non-MBC BLC.

Table 7. Specific Loss of Heterozygosity (LOH) in Medullary Breast Carcinoma (MBC) and Non-MBC Basal-Like Carcinoma (BLC)

Start position	End position	Chromosome	Cytoband	MBC, %	Non-MBC BLC, %
Specific LOH in MBC group (*n* = 19)					
24309700	41814174	2	p23.3-p21	43	15
50184394	50210408	2p	p16.3	42	11

Start position	End position	Chromosome	Cytoband	MBC, %	Non-MBC BLC, %
71779115	71814760	2p	p13.2	42	8
89253701	91,689,680	2p	p11.2-p11.1	42	17
95341388	100168258	2q	q11.1-q11.2	45	17
107002769	114193894	2q	q12.2-q13	57	26
133038729	133114536	2q	q21.2	58	25
52696792	64462524	4q	q11-q13.1	62	30
70982244	71169616	4q	q13.3	63	33
131866907	139609545	4q	q28.3-q31.1	79	50
189263717	190930894	4q	q35.2	89	61
3301088	3370201	7p	p22.2	63	33
16078412	16913789	7p	p21.2-p21.1	63	33
18408294	18807219	7p	p21.1	63	33
55182494	55205930	7p	p11.2	42	17
107591914	107623496	7q	q31.1	42	17
22250879	22392626	14q	q11.2	84	54
20964485	26289925	20p	p11.23-p11.1	45	12
46494273	46889259	20q	q13.3	42	17
62896110	62912463	20q	q13.33	79	25
54491633	54699522	23p	p11.22	68	39
75248351	76230011	23q	q13.3-q21.1	78	47
84224371	96955143	23q	q21.1-q21.33	72	38
Specific LOH in non-MBC BLC group (*n* = 36)					
162270070	162314921	6q	q26	21	50

Start position	End position	Chromosome	Cytoband	MBC, %	Non-MBC BLC, %
1496606	36856268	9p	p24.3-p13.2	19	51
97370455	100817655	11q	q22.1	26	56
114219050	134926754	11q	q23.2-q25	38	74
33612829	47067159	18q	q12.2-q21.1	22	53

Genomic positions are provided according to Human Genome 19 references. Specifi

Figures

Figure 1. Transcriptomic analysis. Hierarchical clustering performed using Average Linkage based on Pearson's dissimilarity of the 679 microarray probe set with an interquartile range >3. Blue signal indicates low expression; red signal, high expression. Histological subtype (first row); large-scale state transition (LST) status of tumor sample (second row); triple-negative breast cancer (TNBC) type according to Lehmann et al.18 (third row); TNBCtype-4 according to Lehmann et al.19 (fourth row). ∗P < 0.05 non-MBC BLC cases in cluster 1 versus versus composition in MBC cases in cluster 2; †P < 0.05, †††P < 0.001 subtype attribution in MBC versus non MBC BLC. BL1, basal-like 1; BL2, basal-like 2; IM, immunomodulatory; LAR, luminal androgen; M, mesenchymal; MSL, mesenchymal stem-like; ND, not determined; UNS, unstable.

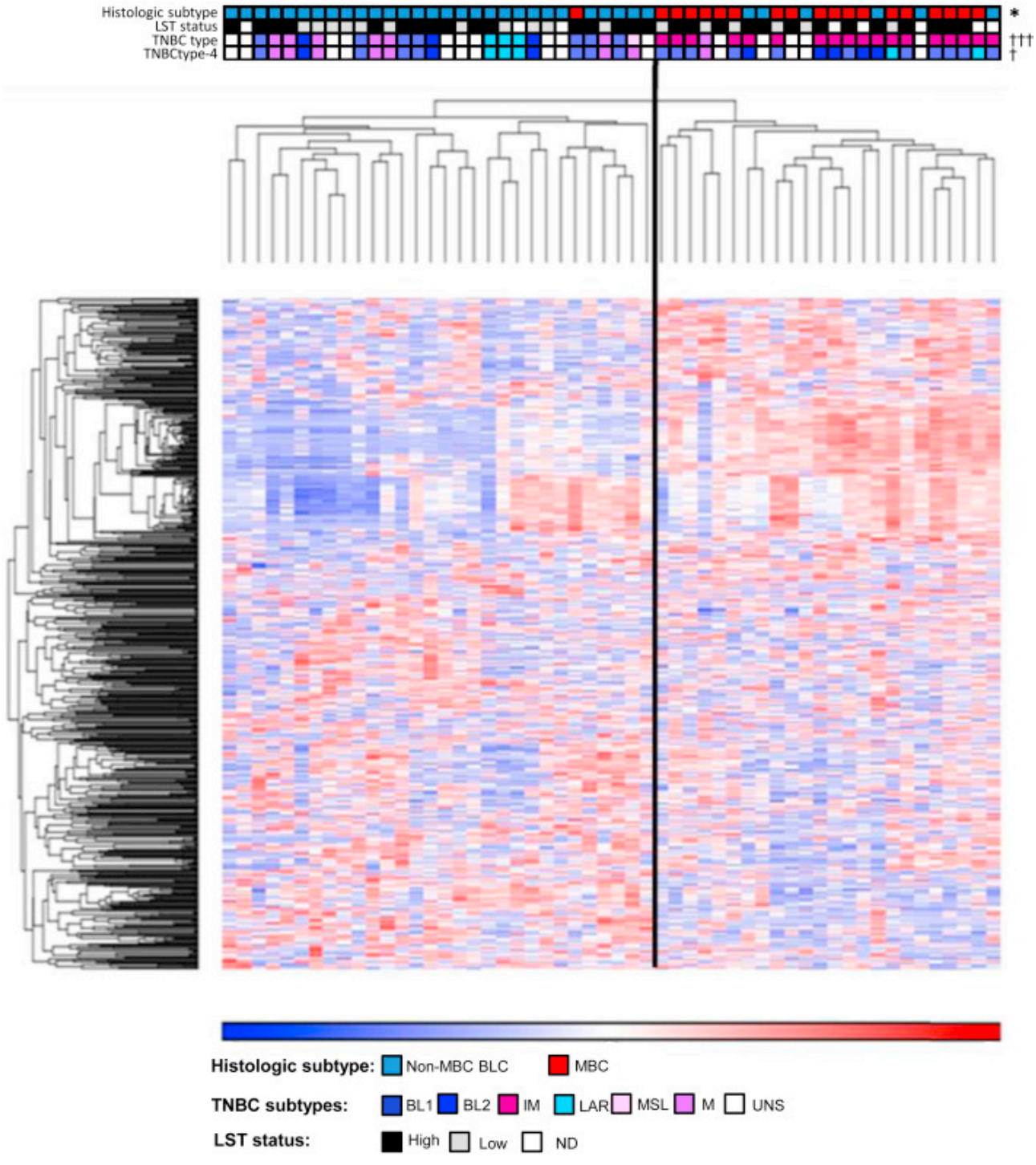

Figure 2. BCLG overexpression in medullary breast carcinoma (MBC). A: Affymetrix U133 Plus 2.0 analysis: BCLG expression level (NBCLG) bar plots in 19 MBCs and 35 non-MBC basal-like carcinomas (BLCs) and corresponding box plots. Red line indicates differential gene expression threshold as defined by the Welch t-test. B: Quantitative RT-PCR validation study: percentage of cases with BCLG overexpression in 19 MBCs, 41 BLCs, and 526 invasive breast carcinomas from different molecular classes. The median NBCLG (range) is given for each group. C: Information on epithelial expression of BCLG: mean human NBCLG in 31 tumor cell lines (and seven nontumor cell lines) (data not shown) and in 61 patient-derived xenografts (PDXs) according to molecular classes. D:BCLG expression by immunohistochemistry in epithelial cancer cells: BCLG staining on MBC formalin-fixed, paraffin-embedded sections. E:BCLG expression by immunohistochemistry in epithelial cancer cells: median BCLG H scores box plots (clone ab184925, Abcam) in 16 MBCs and 27 non-MBC BLCs. F: Spearman linear correlation between BCLG expression level and BCLG H score in MBC and non-MBC BLC. Red line indicates linear regression line (r = 0.328). ∗P < 0.05, ∗∗P < 0.01; †P < 0.05 (Spearmann's rank correlation). Original magnification: ×25 (D, right panel); ×400 (D, left panel).

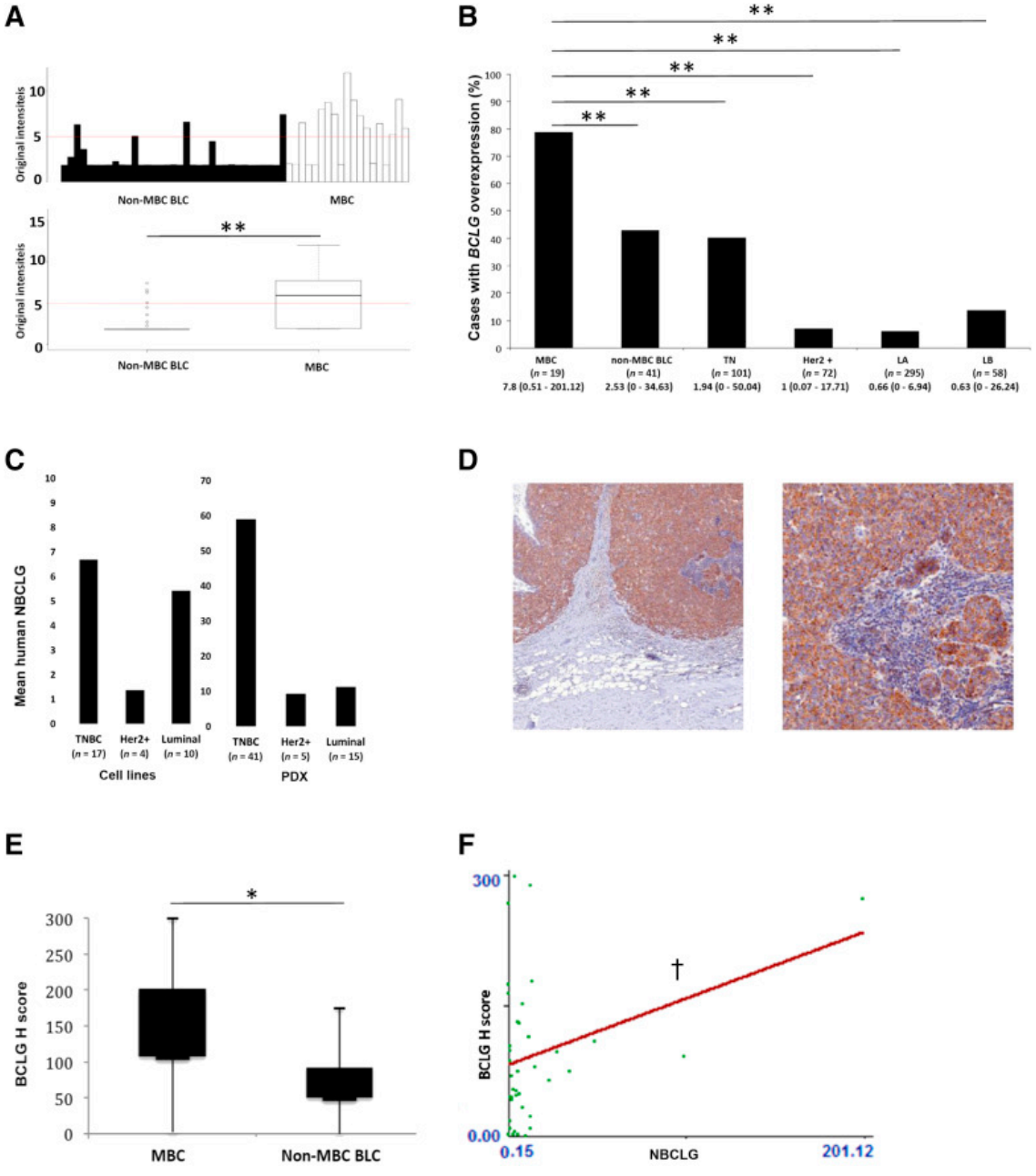

Figure 3. Medullary breast carcinoma (MBC) and non-MBC basal-like carcinoma (BLC) distribution within the transcriptomic classes defined by Lehmann et al.18A: Classification based on six classes. B: Classification based on four classes.19∗P < 0.05, ∗∗∗P < 0.001. BL1, basal-like 1; BL2, basal-like 2; IM, immunomodulatory; LAR, luminal androgen; M, mesenchymal; MSL, mesenchymal stem-like; UNS, unstable.

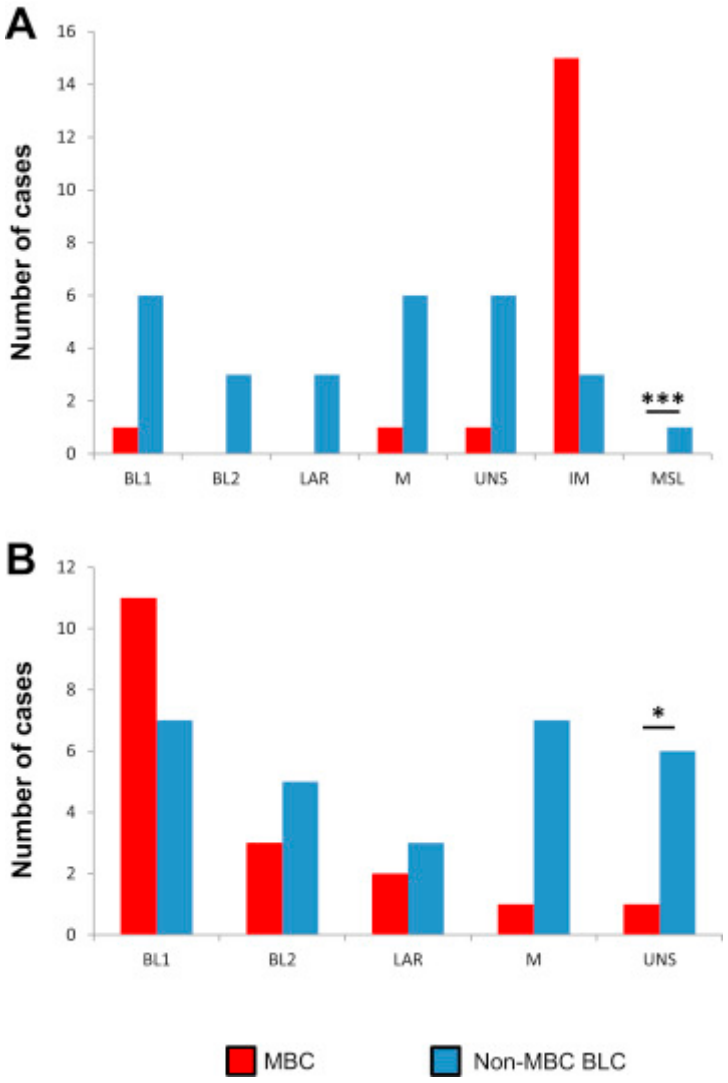

Figure 4. Loss of heterozygosity (LOH) in medullary breast carcinoma (MBC) and non-MBC basal-like carcinoma (BLC). The higher vertical lines indicate chromosome boundaries, the smaller vertical lines indicate centromere boundaries, and horizontal hemidashed lines indicate the 40% frequency threshold. Positive and negative frequencies correspond with frequencies of positive (with gains and copy-neutral) and negative (with losses) LOH.